

Peak positions and shapes in neutron pair correlation functions from powders of highly anisotropic crystals

D. A. Dimitrov, H. Röder, and A. R. Bishop

Los Alamos National Laboratory, Los Alamos, New Mexico 87545

(November 13, 2018)

Abstract

The effect of the powder average on the peak shapes and positions in neutron pair distribution functions of polycrystalline materials is examined. It is shown that for highly anisotropic crystals, the powder average leads to shifts in peak positions and to non-Gaussian peak shapes. The peak shifts can be as large as several percent of the lattice spacing.

61.12.Bt, 61.12.Ld, 63.20.-e

I. INTRODUCTION

The purpose of this paper is to demonstrate that the peak shapes in the powder averaged static pair distribution functions (PDF) of highly anisotropic *harmonic* crystals are generally non-Gaussian and the peak positions (maxima) are at different distances than the average atomic pair distances. Our approach is to consider the effect of the powder average on specific peaks of the theoretical PDF. We discuss the relevance of these results to what is actually measured in neutron diffraction experiments.

The lattice dynamics properties of highly anisotropic crystals, in particular for crystalline materials of layered and chain structure, are known to lead to significant deviations from the Debye approximation for thermodynamic quantities rendering it inapplicable in these cases. Lifshitz¹ showed that there are different low temperature regimes in which the specific heat does not behave as T^3 but rather as T^α with the exponent α having different values depending on the different regimes for the phonon dispersion relations. The behavior of the thermal expansion tensor is similar. The anisotropy also leads to very different in magnitude Debye-Waller factors² and to violation of the Cauchy relations for the elastic constants. The latter is due to the inability to describe the inter-atomic forces with central pair potentials. A number of different models have been developed for the inter-atomic potentials to deal with the anisotropy, depending on the physical properties of the crystal concerned. For example, generalized force constants models are considered for some simple metals, bond bending forces are introduced for the strongly anisotropic covalent crystals, anisotropic ionic polarizabilities for ionic crystals, etc. It is of interest to determine the effects of highly anisotropic harmonic lattice vibrations together with the powder average on the static pair distribution function (PDF) and the implications for the corresponding measurements in neutron powder diffraction experiments.

The space-time pair correlation function $G(\mathbf{r}, t)$ introduced by Van Hove³ in the theory of neutron scattering has been primarily studied, both experimentally and theoretically, for liquids and amorphous materials.⁴ The correlation function in liquids is often assumed

to be Gaussian provided the system is considered as isotropic.^{5,6} The interpretation of the experimental data is quite simplified by assuming Gaussian peaks, and indeed much has been learnt about the structure and the interactions in such systems from the pair correlation function.

The determination of the static PDF from experimental data on powder samples is obtained by first extracting the static structure factor $S(q)$, where $q = |\mathbf{q}|$, from the measured (effective) coherent cross section $\left(\frac{d\sigma_{coh}}{d\Omega}\right)_{eff}$ and then Fourier transforming it. $S(q)$ has structure for large momentum transfers $\hbar q$ in crystals due to their long-range periodic structure. For an accurate PDF to be obtained from the Fourier transform of $S(q)$ in such materials, the structure factor should be known to large enough values of q . Only recently the development of high-intensity neutron sources has allowed the measurement of effective cross sections up to $q \approx 50 \text{ \AA}^{-1}$ or larger and thus the ability to obtain a PDF for polycrystalline materials from neutron diffraction experiments.^{7,8}

The extraction of the structure factor $S(q)$ from the neutron scattering data is based on several assumptions. The first Born approximation is assumed to be applicable for the interpretation of the differential cross section. This is the case, at least in the static approximation when the energy transfer of the scattered particle or photon, in the case of x-rays, is negligible compared to its own energy.³ The static approximation is applicable to the scattering of x-rays but cannot be applied directly to the scattering of neutrons because of their specific energy and wavelength scales (note that the static structure factor $S(\mathbf{q})$ which is obtained by integrating out the ω dependence of $S(\mathbf{q}, \omega)$ is different from the structure factor obtained in the *static approximation*⁹). Corrections to the static approximation have been developed by Placzek¹⁰ and by Wick¹¹ which are applicable for high incident neutron energies. Yarnell *et al.*¹² have shown that the application of the Placzek correction to neutron detectors with different efficiency can lead to determination of the structure factor $S(q)$ with an accuracy of ~ 0.01 for liquid Ar. However, it has been pointed out by Ascarelli and Cagliati¹³ that there are cases when the Placzek correction could lead to large errors, particularly for values of q for which the curvature of $S(q)$ is high. Generally,

this requires a careful study of the Placzek correction before its application is adopted. We shall assume that the Placzek correction is applicable in order to determine the $S(q)$ from the differential scattering cross section, as is usually done when analyzing the experimental data¹⁴ for liquids as well as for crystals.⁸ We also assume that all the other corrections and normalizations applied to the raw data, such as multiple scattering, incoherent scattering calibration, absorption, polarization, etc., and measurements to large momentum transfers are made so that the Fourier transformation termination errors are very small. A careful experimental determination of the PDF which satisfies these assumptions will allow for a meaningful comparison with a theoretical calculation.¹⁵

In Sec. II, we introduce the static pair distribution function for harmonic crystals with arbitrary structure and its relation to the experimental quantities measured. The powder average for specific cases is considered in Sec. III which contains the main results of this paper. The implications of these results together with their relevance to x-ray experiments are discussed in Sec. IV.

II. EXPERIMENTAL AND THEORETICAL BACKGROUND

The coherent differential cross-section for scattering of thermal neutrons in the first Born approximation is given by⁹

$$\left(\frac{d^2\sigma}{d\Omega dE'}\right)_{coh} = \frac{\sigma_{coh}}{4\pi} \frac{k'}{k} \frac{N}{2\pi\hbar} S(\mathbf{q}, \omega), \quad (1)$$

$$S(\mathbf{q}, \omega) = \frac{1}{N} \sum_{j,j'=1}^N \int_{-\infty}^{\infty} \langle e^{-i\mathbf{q}\cdot\mathbf{r}_j(0)} e^{i\mathbf{q}\cdot\mathbf{r}_{j'}(t)} \rangle e^{-i\omega t} dt, \quad (2)$$

where $\sigma_{coh} = 4\pi\bar{b}^2$ (\bar{b} is the compositionally averaged scattering length¹⁶), \mathbf{k} and $\mathbf{k}' = \mathbf{k} - \mathbf{q}$ are the initial and final wave vectors of the scattered neutron, $\mathbf{r}_j(t)$'s are the operators for the position vectors of the N particles in the target system in the Heisenberg representation, $S(\mathbf{q}, \omega)$ is the dynamical structure factor, and $\langle \dots \rangle$ denotes thermal average. We have here

assumed that the scattering system consist of only one type of atoms. In the general case, the different types of atoms will have different scattering lengths and this should modify Eqs. (1) and (2) accordingly. This case will be considered explicitly for the static PDF in crystals.

The Van Hove³ pair distribution function is related to $S(\mathbf{q}, \omega)$ via a space-time Fourier transformation

$$G(\mathbf{r}, t) = \frac{1}{(2\pi)^3} \int S(\mathbf{q}, \omega) e^{-i(\mathbf{q}\cdot\mathbf{r}-\omega t)} d\mathbf{q}d\omega. \quad (3)$$

This function is complex since in the general case the position vector operators for the particles of the scattering system do not commute at different times. At equal times, $t = 0$, these operators commute and $G(\mathbf{r}, 0)$ is real.

Provided $S(\mathbf{q}, \omega)$ can be extracted from the measured differential cross-section, Eq.(1), then Eq. (3) can be used to obtain $G(\mathbf{r}, t)$. The pair distribution function has a simple physical meaning and is easier to understand than $S(\mathbf{q}, \omega)$. It is not currently feasible to determine experimentally the dynamical structure factor in such a domain of the four dimensional (\mathbf{q}, ω) , space for the Fourier transformation in Eq. (3) to be applied. However, in some cases the ω integration can be effectively done by the neutron detectors. This allows for the determination of the static structure factor

$$S(\mathbf{q}) = \int_{-\infty}^{\infty} S(\mathbf{q}, \omega) d\omega = \int G(\mathbf{r}, 0) e^{i\mathbf{q}\cdot\mathbf{r}} d\mathbf{r}, \quad (4)$$

provided \mathbf{q} is kept constant in the ω integration. This is the case, at least, in the static approximation. The neutron detectors carry out this integration at constant scattering angle θ and the effective coherent cross-section per unit solid angle is

$$\left(\frac{d\sigma}{d\Omega}\right)_{coh}^{eff} = \frac{\sigma_{coh}}{4\pi} \frac{N}{2\pi\hbar} \int_{-\infty}^{\omega_{max}} \epsilon(k') \frac{k'}{k} S(\mathbf{q}, \omega) d\omega, \quad (5)$$

where $\hbar\omega_{max}$ is the energy of the incoming neutron, $\epsilon(k')$ is the detector's energy dependent efficiency, and \mathbf{q} is a function of the scattering angle θ via $q^2 = k^2 + k'^2 - 2kk' \cos(2\theta)$. The problem is to obtain $S(\mathbf{q})$, as defined by Eq. (4), from the measured effective cross section

$(\frac{d\sigma}{d\Omega})_{coh}^{eff}$ when the static approximation is not valid. The usual way to tackle this problem is to apply the Placzek correction as mentioned in Sec. I, particularly when the incident neutron energy is high compared to the energy transfers in the scattering processes.

For powder samples, the correlation functions do not depend on the angular coordinates of \mathbf{q} and \mathbf{r} since they are effectively averaged over these variables. Then the relations between $S(q)$ and

$$\rho(r) = G(r, 0) - \delta(r) \quad (6)$$

are

$$q(S(q) - 1) = 4\pi \int_0^\infty (\rho(r) - \rho_0) r \sin(qr) dr, \quad (7)$$

$$r(\rho(r) - \rho_0) = \frac{1}{2\pi^2} \int_0^\infty (S(q) - 1) q \sin(qr) dq, \quad (8)$$

where $\rho_0 = N/V$, V is the volume of the system, and the forward scattering has been subtracted from $S(q)$, which is the conventional practice since it is negligible for scattering angles larger than $\sim 10^{-2}$ seconds of arc.¹² The experimental PDF, $\rho_{exp}(r)$, is obtained from Eq. (8) with the upper limit of the integration $q = q_{max}$ determined from the maximum value of the scattering vector accessible in the measurement. If the assumptions made in Sec. I regarding $\rho_{exp}(r)$ are valid, we can compare this with a theoretically derived $\rho(r)$ which we consider next for harmonic crystals.

The static pair distribution function, $\rho(\mathbf{r})$, in a form suitable for neutron diffraction from a crystal can be defined by

$$\rho(\mathbf{r}) = \frac{1}{N_b} \sum_{\mathbf{R}(l'), d, d'} \frac{b(0d)b(l'd')}{\bar{b}^2} \langle \delta(\mathbf{r} - \mathbf{r}(0d; l'd')) \rangle, \quad (9)$$

where N_b is the number of basis atoms in the unit cell, $\mathbf{R}(l)$ is the position vector of the origin of the l th unit cell, d, d' are basis atom indices, $b(ld)$ is the scattering length of the atom with equilibrium position at $\mathbf{R}(ld) = \mathbf{R}(l) + \mathbf{R}(d)$. $\mathbf{R}(d)$ is the position vector of the d th atom in the basis relative to the origin of the cell. The $\mathbf{r}(0d; l'd') = \mathbf{r}(0d) - \mathbf{r}(l'd')$

is the difference between the instantaneous positions of the two atoms. The instantaneous position of an atom is $\mathbf{r}(ld) = \mathbf{R}(ld) + \mathbf{u}(ld)$, where $\mathbf{u}(ld)$ is the deviation vector from the equilibrium position (the time arguments of the two \mathbf{u} vectors in Eq.(9) are not explicitly written since they are at equal times). The sum excludes the terms with $l' = 0$, and $d = d'$. For harmonic crystals

$$\rho(\mathbf{r}) = \frac{1}{N_b} \sum_{\mathbf{R}(l',d,d')} \frac{b(0d)b(l'd')}{\bar{b}^2} \times \frac{e^{-\frac{1}{2}(\mathbf{r}-\mathbf{R}(0d;l'd')) \cdot \mathcal{T}^{-1}(0d;l'd') \cdot (\mathbf{r}-\mathbf{R}(0d;l'd'))}}{\sqrt{(2\pi)^3 \det [\mathcal{T}(0d;l'd')]}} \quad (10)$$

where $\mathbf{R}(0d;l'd') = \mathbf{R}(0d) - \mathbf{R}(l'd')$, and the tensor $\mathcal{T}(0d;l'd')$ is

$$\mathcal{T}_{\alpha\beta}(0d;l'd') = \left\langle (\mathbf{u}(0d) - \mathbf{u}(l'd'))_{\alpha} (\mathbf{u}(0d) - \mathbf{u}(l'd'))_{\beta} \right\rangle. \quad (11)$$

The result for $G(\mathbf{r}, t)$, $t \neq 0$, in such crystals is given by Van Hove.³ The thermodynamic averages of the type $\langle \mathbf{u}_{\alpha}(ld) \mathbf{u}_{\beta}(l'd') \rangle$ are easily evaluated once the phonon frequencies $\omega_s(\mathbf{k})$ and polarization vectors $\boldsymbol{\sigma}_d^s(\mathbf{k})$, where s is the branch index, are known for reciprocal space \mathbf{k} -vectors in the first Brillouin zone

$$\langle \mathbf{u}_{\alpha}(ld) \mathbf{u}_{\beta}(l'd') \rangle = \frac{\hbar}{2N_k \sqrt{M_d M_{d'}}} \sum_{\mathbf{k},s} e^{i\mathbf{k} \cdot (\mathbf{R}(l) - \mathbf{R}(l'))} \boldsymbol{\sigma}_{d\alpha}^s(\mathbf{k}) \boldsymbol{\sigma}_{d'\beta}^{s*}(\mathbf{k}) \frac{(2n_s(\mathbf{k}) + 1)}{\omega_s(\mathbf{k})}. \quad (12)$$

Here $n_s(\mathbf{k}) = (\exp(\beta\hbar\omega_s(\mathbf{k})) - 1)^{-1}$, N_k is the number of unit cells in a crystal with periodic boundary conditions (or k points in the first Brillouin zone), and M_d is the mass of the d th type of atom. Note that $\langle \mathbf{u}_{\alpha}(ld) \mathbf{u}_{\beta}(ld) \rangle$ is related to the Debye-Waller¹⁶ factor via $2W_d(\mathbf{q}) = \mathbf{q} \cdot \langle \mathbf{u}(ld) \mathbf{u}(ld) \rangle \cdot \mathbf{q}$, where \mathbf{q} is a reciprocal space vector.

As expected, the static PDF for harmonic crystals as a function of the vector argument \mathbf{r} , Eq. (10), consists of a sum of Gaussian distributions for each pair of atoms, apart from the scattering length factors. Each distribution is centered at the pair's average distance $\mathbf{R}(0d;l'd')$ and its second moments with respect to $\mathbf{R}(0d;l'd')$ are given by the elements of the tensor $\mathcal{T}(0d;l'd')$. These moments determine the width of the peaks in the PDF along

any direction in \mathbf{r} -space. It is clear from Eq. (12) that the moments depend on $\mathbf{R}(l) - \mathbf{R}(l')$ and the type of atoms in the pair. Since $\langle \mathbf{u}_\alpha(ld) \mathbf{u}_\beta(l'd') \rangle \rightarrow 0$ when $|\mathbf{R}(l) - \mathbf{R}(l')| \rightarrow \infty$, the moments of the distribution will approach $\langle \mathbf{u}_\alpha(0d) \mathbf{u}_\beta(0d) \rangle + \langle \mathbf{u}_\alpha(0d') \mathbf{u}_\beta(0d') \rangle$ and will become distance independent in this limit.

III. POWDER AVERAGE

When the scattering is from a crystalline powder sample, the structure factor depends only on the magnitude of the scattering vector and is averaged over its angular coordinates. Then the pair distribution function defined by Eq. (3), or by the inverse Fourier transform of Eq. (4) for the static PDF, will depend only on r and not on the direction of \mathbf{r} . In the latter case, this is equivalent to an angular average in real space

$$\rho(r) = \int_{S_{\Omega_r}} \frac{d\Omega_r}{4\pi} \rho(\mathbf{r}), \quad (13)$$

where $r \equiv |\mathbf{r}|$ and S_{Ω_r} is the surface of a sphere with a center at the origin of the coordinate system and a radius r . The static, angularly averaged, $S(q)$ and $\rho(r)$ are related by Eqs. (7) and (8).

Below, we will apply Eq. (13) to the different peaks in $\rho(\mathbf{r})$, as given for crystals by Eq. (10), in order to examine the effects of the powder average on the static PDF. Note that if $\rho(r)$ is to be obtained from $S(q)$ via Eq. (8), the integral over q must be carried out to infinity rather than to a maximum value q_{max} determined by the scattering instrument. In what follows, it is understood that the assumptions made in Sec. I hold such that the theoretical PDF obtained from Eqs. (10) and (13) can be compared with the experimentally determined.

We consider first the case of an isotropic tensor $\mathcal{T}(0d; l'd')$ because it is an important limiting case against which we can compare the case of a general form of \mathcal{T} .

A. Gaussian Behavior of $r\rho(r)$ Peaks

The simplest case for which the powder average integral, Eq.(13), can be taken analytically is for an atomic pair with an isotropic $\mathcal{T}(0d; l'd') = t^2\mathcal{I}$ tensor (note that generally in taking the integral in Eq.(13) for each pair, the \mathbf{r} -space coordinate system can always be rotated such that $\mathcal{T}(0d; l'd') = \text{diag}\{t_1^2, t_2^2, t_3^2\}$), where \mathcal{I} is the identity tensor. The contribution $\rho_{(0d; l'd')}(r)$ of such a pair to the total PDF is

$$\rho_{(0d; l'd')}(r) = \frac{b(0d)b(l'd')}{\bar{b}^2 4\pi r R(0d; l'd')} (p_{N(R(0d; l'd'), t^2)}(r) - p_{N(-R(0d; l'd'), t^2)}(r)), \quad (14)$$

where $p_{N(R, t^2)}(r) = e^{-(r-R)^2/2t^2} / \sqrt{2\pi t^2}$ is the density of the normal distribution with a mean equal to R and standard deviation t . The contribution of $p_{N(-R(0d; l'd'), t^2)}(r)$ to the PDF can often be neglected when t^2 is large enough, and for r of the order of the pair distances in a crystalline solid which are usually equal to several Angstroms or larger. Then the peak in $r\rho(r)$ due to such a pair of atoms will be approximately a Gaussian (centered at the equilibrium distance $R(0d; l'd')$ between the atoms and with a standard deviation equal to t) divided by $R(0d; l'd')$ (apart from the constant scattering length factor $b(0d)b(l'd')/4\pi\bar{b}^2$). Therefore, if for all pairs $\mathcal{T}(0d; l'd') = t^2(0d; l'd')\mathcal{I}$ were isotropic (which is *not* the case for crystalline solids) the powder averaged PDF would be

$$\rho(r) \approx \frac{1}{N_b} \sum_{\mathbf{R}(l', d, d')} \frac{b(0d)b(l'd')}{\bar{b}^2 4\pi r} \frac{p_{N(R(0d; l'd'), t^2(0d; l'd'))}(r)}{R(0d; l'd')}. \quad (15)$$

Strictly, $4\pi r\rho(r)$ is not a sum of Gaussians (again neglecting the scattering length factors) since each $p_{N(R(0d; l'd'), t^2(0d; l'd'))}(r)$ is also scaled by its mean value $R(0d; l'd')$ which is different for the pairs nonequivalent by symmetry. The form for an isotropic PDF peak given by Eq.(14) can be used to approximate peaks in diagonally cubic crystals¹⁷ when

$$|\langle \mathbf{u}_\alpha(0d)\mathbf{u}_\beta(l'd') \rangle + \langle \mathbf{u}_\alpha(l'd')\mathbf{u}_\beta(0d) \rangle| \ll u^2(0d) + u^2(l'd'),$$

for $\alpha, \beta = x, y, z$, since in such crystals $\langle \mathbf{u}(ld)\mathbf{u}(ld) \rangle = u^2(ld)\mathcal{I}$. This may be applicable to pairs of atoms separated by a large distance relative to the nearest neighbor distance

such that the correlation terms become much smaller than the diagonal elements of the self correlation ones. This is a special case of the more general statement that the long-range part of the PDF can be obtained to a very good approximation only from the Fourier transformation of the elastic part of $S(q)$.

B. Non-Gaussian Behavior of $r\rho(r)$ Peaks

We consider next a case which allows us to study the effect of the powder average for a strongly anisotropic tensor \mathcal{T} and which can still be handled analytically. The powder average contribution to the PDF due to a pair of atoms with $\mathcal{T}(0d; l'd') = \text{diag} \{t_{\perp}^2, t_{\perp}^2, t_{\parallel}^2\}$, $t_{\parallel}^2 < t_{\perp}^2$, and $\mathbf{R}(0d; l'd') = (0, 0, R)$ is

$$\rho_{(0d;l'd')} (r) = \frac{1}{4\pi r} \left(p_{N(R,t_{\parallel}^2)}(r)G(ar - bR) + p_{N(-R,t_{\parallel}^2)}(r)G(ar + bR) \right), \quad (16)$$

where

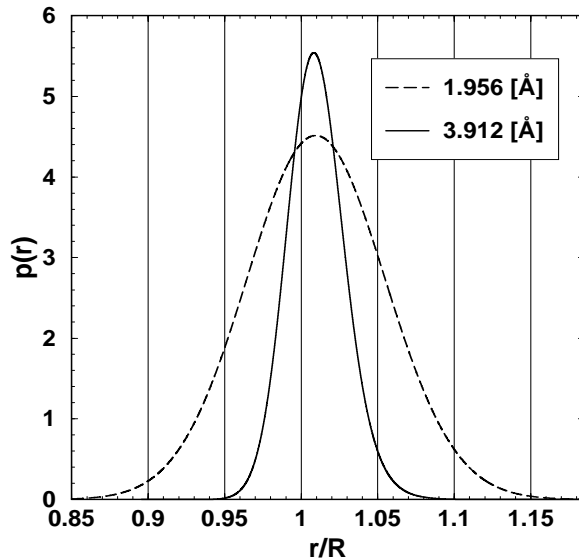
$$G(x) = \sqrt{\pi t_{\parallel}^2 / 2t_{\perp}^2 (t_{\perp}^2 - t_{\parallel}^2)} \exp(x^2) \text{erf}(x),$$

$a = \sqrt{(t_{\perp}^2 - t_{\parallel}^2) / 2t_{\perp}^2 t_{\parallel}^2}$, $b = \sqrt{t_{\perp}^2 / 2t_{\parallel}^2 (t_{\perp}^2 - t_{\parallel}^2)}$, $\text{erf}(x)$ is the error function, and we have omitted the scattering lengths scaling factor $b(0d)b(l'd')/\bar{b}^2$. It is straightforward to check that in the limit $t_{\parallel}^2 \rightarrow t_{\perp}^2$ from below we recover the result for the isotropic case given by Eq.(14). These specific forms of \mathcal{T} and \mathbf{R} arise, for example, for specific $O_{\text{I}}-B$ or $O_{\text{I}}-O_{\text{I}}$ nearest neighbor pairs of atoms in ABO_3 cubic perovskites. We use here Cowley's notation¹⁸ for this structure. The self correlation term $\langle \mathbf{u}(B)\mathbf{u}(B) \rangle$ for the B atoms is isotropic and the anisotropy in the \mathcal{T} is due to the oxygen self correlation term. The latter is proportional to its Debye-Waller factor and has the same form as \mathcal{T} . The $B-O$ correlation terms also contribute to increasing the anisotropy of \mathcal{T} . For the $O_{\text{I}}-O_{\text{I}}$ pair of atoms, the \mathcal{T} tensor is even more anisotropic because of the contributions of both atom's anisotropic $\langle \mathbf{u}(O_{\text{I}})\mathbf{u}(O_{\text{I}}) \rangle$ terms. Physically, this is associated with the local environment of the O_{I} atom. It has four A nearest neighbors (nn) in the xy plane and two nn B atoms along the z axis. The oxygen

polarizability is also very anisotropic and it depends strongly on the oxygen's environment.¹⁹ To study the peak positions and shapes as functions of t_{\perp}^2 and t_{\parallel}^2 we have chosen $R = 1.956$ and $R = 3.912 \text{ \AA}$ (the lattice constant in cubic ABO_3 perovskites is often close to 3.9 \AA) which corresponds to the first nearest neighbor O_I-B and O_I-O_I bond distances. The t_{\perp}^2 , t_{\parallel}^2 are varied in intervals such that $5 \leq t_{\perp}^{-2} \leq 99 \text{ \AA}^{-2}$ and $100 \leq t_{\parallel}^{-2} \leq 250 \text{ \AA}^{-2}$. Lattice dynamics calculations²⁰ on $\text{La}_{0.7}\text{Sr}_{0.3}\text{MnO}_3$ using the cubic perovskite structure and the nonlinear shell model of Migoni *et al.*¹⁹ show that these intervals for t_{\perp}^2 , t_{\parallel}^2 could be physically relevant. The peaks of the normalized (to unity) distributions $p(r) = \text{Const} \times r \rho_R(r)$ for two $(R, t_{\perp}^{-2}, t_{\parallel}^{-2})$ sets of parameters, $(1.956, 21.71, 133.99)$ and $(3.912, 6.23, 248.11)$, are shown in Fig. 1. These values of $(R, t_{\perp}^{-2}, t_{\parallel}^{-2})$ arise for a specific set of the shell model parameters chosen from a Monte Carlo sample sequence in a domain of their phase space. The sequence was generated in a Reverse Monte Carlo estimation¹⁵ of the shell model parameters from PDF data.²⁰

FIGURES

FIG. 1. Non Gaussian peaks in the normalized distribution of $r\rho_R(r)$ vs r/R for two values of $(R, t_{\perp}^{-2}, t_{\parallel}^{-2})$. The magnitudes of R are given in the inset of the figure. Each peak position is shifted at a value greater than the corresponding average distance R .



We calculated these peaks using a numerical implementation of Eq. (16) with a step in r equal to 10^{-4} Å. The maximum of each peak (its position) is shifted to a distance larger than the corresponding average R . This shift is equal to 0.0186 Å for the peak with $R = 1.956$ Å and to 0.0321 Å for the one with $R = 3.912$ Å. These are fairly large peak shifts and, importantly, of the same magnitude as observed peak shifts in specific materials interpreted as statistic displacements from the periodic lattice structure. The peak shapes show deviation from the Gaussian, as the asymmetry in the shape with respect to the peak position is clear from the figure (a quantitative measure for this will be given below). The $p(r)$ decreases to zero slower for $r > R_{max}$, where R_{max} is the distance of the peak position, than for $r < R_{max}$.

It is of interest to note a recent study²¹ on the PDF of the superconducting $\text{La}_{2-x}\text{Sr}_x\text{CuO}_4$ in which a change of the Cu-O bond length equal to 0.024 Å was reported. However, this bond change has been attributed to a different mechanism. This is a layered material and it will clearly be of importance to be able to estimate to what extent this shift may actually

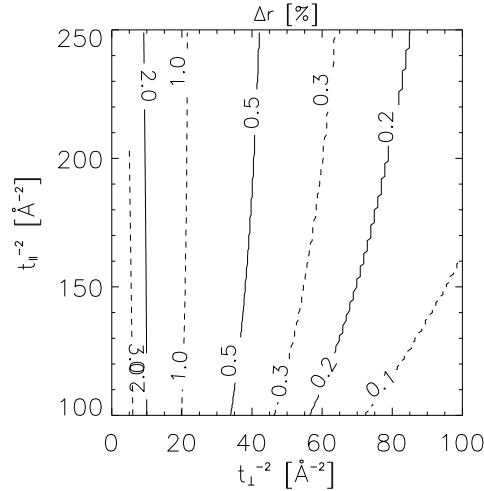
be due to the effect of the powder average.

We proceed to formally study the peak shift relative to the average R and the deviation of the peak shape from the Gaussian for the domain of $(t_{\perp}^{-2}, t_{\parallel}^{-2})$ given above and for $R = 1.956 \text{ \AA}$. The peak shift

$$\Delta r = \frac{R_{max} - R}{R} \times 100, \quad (17)$$

change relative to the average distance between the atoms in the pair is plotted as a function of t_{\perp}^{-2} and t_{\parallel}^{-2} in Fig 2.

FIG. 2. Contour plot of the peak shift magnitude, Eq.(17) as a function of the t_{\perp}^{-2} and t_{\parallel}^{-2} parameters.



The figure shows that increasing the anisotropy of the eigenvalues of the \mathcal{T} tensor could lead to peak shifts as large as 3% of R . Moreover, the contour plot gives that for shifts larger than approximately 0.5%, the value of the t_{\perp}^{-2} remains almost unchanged on each contour level while increasing t_{\parallel}^{-2} . Note that peak shifts of the order of 0.5% ($\approx 0.01 \text{ \AA}$ for $R = 1.97 \text{ \AA}$) or larger should not be difficult to detect experimentally. In the limit $t_{\perp}^{-2} \rightarrow t_{\parallel}^{-2}$ from below, the peak shift tends to zero as it should in the isotropic limit and the peak position is at the average distance R .

The deviation of a peak in $r\rho(r)$ from a Gaussian form can be studied²² by calculating the moments of the normalized (to unity) distribution given by this peak. If the normalized

distribution were a Gaussian $p_{N(\bar{r},\sigma^2)}$, the moments obey

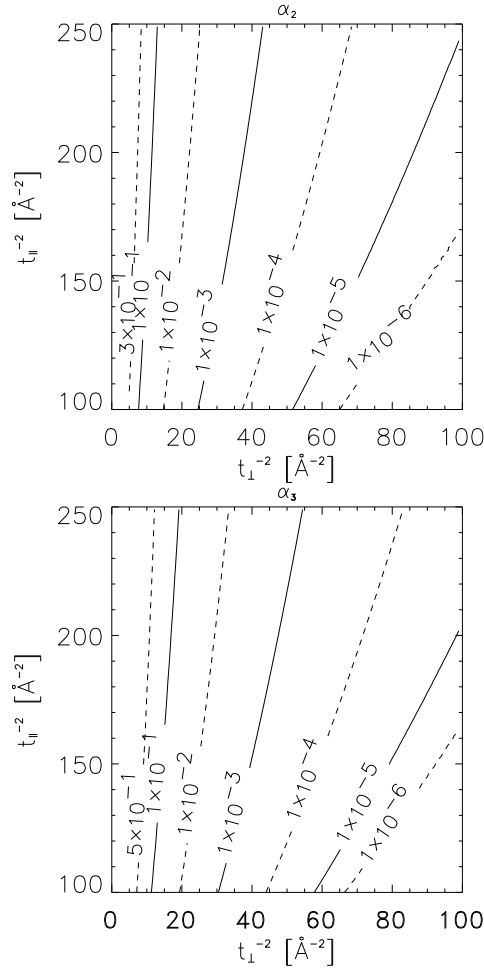
$$\begin{aligned}\overline{(r - \bar{r})^{2n-1}} &= 0, \\ \overline{(r - \bar{r})^{2n}} &= (2n - 1)!! \left(\overline{(r - \bar{r})^2} \right)^n,\end{aligned}$$

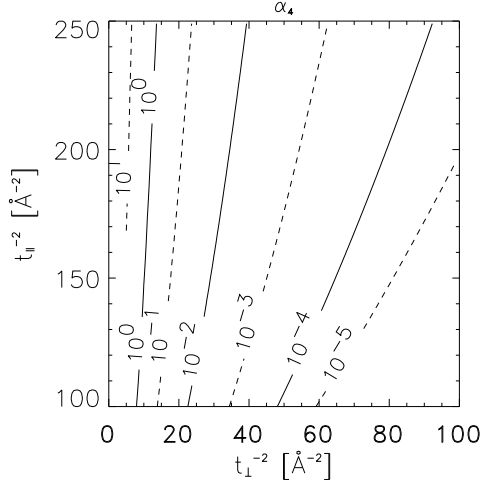
for $n = 1, 2, \dots$. When the normalized distribution deviates from a Gaussian, the quantity

$$\alpha_n = \frac{\overline{(r - \bar{r})^{2n}}}{(2n - 1)!! \left(\overline{(r - \bar{r})^2} \right)^n} - 1, \quad n = 2, 3, \dots, \quad (18)$$

will deviate from zero. The contour plots of the dependence of α_n ($n = 2, 3, 4$) on $(t_{\parallel}^{-2}, t_{\perp}^{-2})$ for the same intervals as in Fig. 2 and for the same peak is given in Fig. 3.

FIG. 3. Contour plots of the dependence of α_n , ($n = 2, 3, 4$) (see Eq.(18)) on $(t_{\parallel}^{-2}, t_{\perp}^{-2})$ for the same peak as in Fig. 2.





The behavior of α_n ($n = 2, 3, 4$) as a function of $(t_{\parallel}^{-2}, t_{\perp}^{-2})$ is very similar to the behavior of the peak shift shown in Fig. 2, as expected. When \mathcal{T} is close to isotropic the peak shift is less than 0.1%, Figs. 2 and 3, which is $\leq 0.002 \text{ \AA}$ for this peak, and the peak shape is close to a Gaussian ($\alpha_n < 10^{-5}$, $n = 2, 3, 4$). The values of α_2 , α_3 , and α_4 are all positive for these intervals of t_{\parallel}^{-2} and t_{\perp}^{-2} indicating that the normalized distribution of $r\rho(r)$ for this peak tends to zero slower than a Gaussian with increasing r .

The magnitude of the peak shift and the behavior of the α_n quantities plotted in Fig. 2 and Fig. 3 depend on the anisotropy of the tensor \mathcal{T} , e.g. determined by the ratio of its largest to smallest eigenvalues, and on the average pair distance R . Fig. 2 shows that for $t_{\perp}^{-2} < 40 \text{ \AA}^{-2}$, the peak position shift is approximately constant for a constant t_{\perp}^{-2} and varying t_{\parallel}^{-2} . Thus, the peak shift of 0.82 % for the peak with $R = 1.956 \text{ \AA}$ plotted in Fig. 1 and a ratio of $t_{\parallel}^{-2}/t_{\perp}^{-2} \approx 6.17$ could be obtained for the same R and $t_{\parallel}^{-2}/t_{\perp}^{-2} \approx 4$. Such ratios, and even much larger, have been experimentally observed at least for the self-correlation tensors $\langle \mathbf{u}\mathbf{u} \rangle$, as can be seen from published Debye-Waller factors in highly anisotropic materials. For example, $\langle u_{\parallel}^2 \rangle / \langle u_{\perp}^2 \rangle \approx 3$ has been found for layered graphite crystals²³ and $\langle u_x^2 \rangle / \langle u_z^2 \rangle \approx 19$ for the monoclinic 7M structure²⁴ in $\text{Ni}_{62.5}\text{Al}_{37.5}$.

The peak shift for a peak given by Eq. (16) decreases when increasing R . This shift was 0.0186 \AA for the peak due to the $O_{\text{I}}\text{-}B$ nn pair of atoms, $(R, t_{\perp}^{-2}, t_{\parallel}^{-2}) = (1.956, 21.71, 133.99)$, and it reaches 0.001 \AA for $R \approx 37 \text{ \AA}$ and the same values of $(t_{\perp}^{-2}, t_{\parallel}^{-2})$.

While the eigenvalues of the \mathcal{T} tensor will also change with R due to the pair displacement correlation contributions to \mathcal{T} , these contributions will decrease with increasing R and for large distances, the eigenvalues of \mathcal{T} will be approximately given by the displacement-displacement self correlations. Then for very anisotropic Debye-Waller factors \mathcal{T} will also be very anisotropic and peak shifts will result for the powder average. More importantly, these shifts will be different for the atomic pairs at different distances with shifts as large as e.g. 0.02 Å for the nn bonds and decreasing slowly to 0.001 Å for $R \approx 37$ Å. Moreover, these shifts are confined to the pairs in which at least one of the atoms is O, in our perovskite example, while peaks due to A-A or B-B pairs could be positioned very close to their respective average R 's at all distances, because for these atoms the Debye-Waller factors are very close to isotropic. Thus, we may have a crystal with several different types of atoms in the unit cell, very well defined periodic structure, and nevertheless some of the peak positions in its powder averaged PDF could deviate one or more percent from the average atomic pair distances while other peaks could be practically positioned, within the resolution in r space, at the average R 's.

IV. SUMMARY

We have considered the effect of the powder average on the peak shapes and positions of the pair distribution function as measured from neutron diffraction, assuming that the harmonic approximation is a valid description for the phonons in the system. When the pair correlation displacement tensor $\mathcal{T}(ld; l'd')$ for a given pair of atoms is isotropic the shape of the peak in $r\rho(r)$ (and *not* in $\rho(r)$) corresponding to this pair is a Gaussian scaled by the average distance $R(ld; l'd')$ between the atoms and a factor which depends on the scattering lengths. However, for polycrystalline samples, the pair correlation tensor $\mathcal{T}(ld; l'd')$ is generally not isotropic. Then the powder average leads to deviations from the Gaussian shape and to peak shifts depending on the “degree of anisotropy” of \mathcal{T} and the magnitude of the average distance R . The anisotropy of \mathcal{T} depends on the relative magnitude of its

eigenvalues. For the specific \mathcal{T} and \mathbf{R} of a pair of atoms, the magnitude of the peak shift can be as large as several percent of the magnitude of the average pair distance R . This could be of the order of 0.02 \AA or larger. Such a change in a peak position should be possible to detect experimentally given the currently available, high resolution neutron diffraction measurements using high intensity neutron pulse sources. Analysis of the moments of the normalized distribution of a peak in $r\rho(r)$ on the anisotropy of \mathcal{T} shows that the normalized distribution tends to zero slower than a Gaussian for increasing r . It is also possible to have a highly anisotropic material for which some of the peaks in its powder averaged PDF are displaced markedly from the average positions while other peaks are at their atomic pairs average distances. In this case, the Rietveld analysis of the Bragg peaks may show that the crystal is periodic.

Generally, for any experiment which allows to obtain the powder averaged $\rho(r)$ accurately enough for (perfect) harmonic crystals in order to make a meaningful comparison with the theoretical PDF as obtained from Eqs. (10) and (13), the peak shifts and shapes reported here should be relevant effects. We considered in this paper the case of neutron powder diffraction experiments which we expect to be an appropriate probe to detect the peak shape and position effects we predict based on the theoretical results. Other experiments which allow to probe the PDF of a polycrystalline material are x-ray scattering and EXAFS.²⁵ Similarly to the neutron experiments, a structure factor can be deduced from x-ray scattering data. In principle, from its inversion (Eq. (8)), a PDF can be obtained. This is, however, more complicated for x-rays than for neutrons since the scattering lengths for x-rays (the atomic form factors) are q -dependent rather than just numbers in the case of neutrons. Powder averaged PDF are often used in the interpretation of EXAFS spectra but Gaussian peaks are assumed at the average distances.

Clearly, experimental confirmation of our result will be very important for the proper analysis and understanding of PDF data in very anisotropic materials.

Work at Los Alamos is supported by the Department of Energy under contract W-7405-ENG-36.

ACKNOWLEDGEMENTS

D. A. Dimitrov would like to express his gratitude to Professors T. Egami and D. Louca for valuable discussions regarding the neutron diffractoin PDF experiments.

REFERENCES

- ¹ I. M. Lifshitz, Zh. Eksp. Teor. Fiz. **22**, 475 (1952).
- ² M. A. Krivoglaz and A. V. Min'kov, Sov. Phys. Crystallogr. **27**, 503 (1982) and the references therein.
- ³ L. Van Hove, Phys. Rev. **95**, 249 (1954).
- ⁴ Y. Waseda, *The Structure of Non-Crystalline Materials* (McGraw-Hill, New York, 1980).
- ⁵ A. Rahman, K. S. Singwi, and A. Sjölander, Phys. Rev. **126**, 986 (1962). This paper approximates the self correlation function $G_s(r, t)$ with a Gaussian which is justified for very short and long times.
- ⁶ R. Kaplow, S. L. Strong, and B. L. Averbach, Phys. Rev. **138**, A 1336 (1965). The radial distribution function obtained from X-ray diffraction scattering data is modeled with gaussians.
- ⁷ T. Egami, Mater. Trans. **31**, 163 (1990).
- ⁸ B. H. Toby and T. Egami, Acta Cryst. A **48**, 336 (1991).
- ⁹ See, e.g., G. L. Squires, *Introduction to the Theory of Thermal Neutron Scattering* (Cambridge University Press, New York, 1978).
- ¹⁰ G. Placzek, Phys. Rev. **86**, 377 (1952).
- ¹¹ G. C. Wick, Phys. Rev. **94**, 1228 (1954).
- ¹² J. L. Yarnell, M. J. Katz, R. G. Wenzel, and S. H. Koenig, Phys. Rev. A **7**, 2130 (1973).
- ¹³ P. Ascarelli and G. Caglioti, Nuovo Cimento **43B**, 376 (1966).
- ¹⁴ P. A. Egelstaff, in *Methods of Experimental Physics* v. 23, Part B, *Neutron Scattering*, edited by D. L. Price and K. Sköld (Academic Press, San Diego, 1987).
- ¹⁵ D. A. Dimitrov, D. Louca, and Röder, Phys. Rev. B **60**, 6204 (1999).

- ¹⁶ S. W. Lovesey, *Theory of Neutron Scattering from Condensed Matter* (Clarendon Press, Oxford, 1985), v. 1.
- ¹⁷ M. Born and K. Huang, *Dynamical Theory of Crystal Lattices*, (Oxford University Press, Oxford, England, 1954).
- ¹⁸ R. A. Cowley, Phys. Rev. B **134**, A981 (1964).
- ¹⁹ R. Migoni, H. Bilz, and D. Bäuerle, Phys. Rev. Lett. **37**, 1155 (1976).
- ²⁰ D. A. Dimitrov, H. Röder, D. Louca, unpublished.
- ²¹ E. S. Bozin, G. H. Kwei, H. Takagi, and S. J. L. Billinge, Phys. Rev. Lett. **84**, 5856 (2000).
- ²² A. Rahman, Phys. Rev. A **136**, 405 (1964).
- ²³ G. Albinet, J. P. Biberian, and M. Bienfait, Phys. Rev. B **71**, 2015 (1971); Von A. Ludsteck, Acta Cryst. **A28**, 59 (1972); J. P. Biberian and M. Bienfait, Acta Cryst. **A29**, 221 (1973).
- ²⁴ Y. Noda, S. M. Shapiro, G. Shirane, Y. Yamada, and L. E. Tanner, Phys. Rev. B **42**, 10397 (1990).
- ²⁵ *X-Ray Absorption, Principles, Applications, Techniques of EXAFS, SEXAFS and XANES*, edited by D. C. Konigsberger and R. Prins (Wiley, New York, 1988).